Research Article | Vol. 25, No. 6 | 20 Mar 2017 | OPTICS EXPRESS 6690

Optics EXPRESS

Spectral phase noise analysis of a cryogenically cooled Ti:Sapphire amplifier

R. S. NAGYMIHALY,[1,2,*] P. JOJART,[1,2] A. BORZSONYI,[1,2] AND K. OSVAY[1]

[1]*ELI-HU Non-Profit Ltd., Dugonics tér 13, Szeged, Hungary*
[2]*Department of Optics and Quantum Electronics, University of Szeged, P.O. Box 406, H-6701 Szeged, Hungary*
[*]*Roland.Nagymihaly@eli-alps.hu*

Abstract: The spectral phase noise of a cryogenically cooled Ti:Sapphire amplifier was analyzed by spectrally resolved interferometry. Since a relative phase difference measurement is performed, the effect of the amplifier stage can be determined with high precision. Contributions of the cooling system to the spectral phase noise were found to be below 50 mrad for both the vacuum pumps and the cryogenic system. The carrier-envelope phase noise of thermal and mechanical origin was also determined for different repetition rates of laser operation. Mechanical vibrational spectra were recorded by an accelerometer for different stages of operation and compared to the interferometric phase noise measurements.

OCIS codes: (140.7090) Ultrafast lasers; (140.3280) Laser amplifiers; (140.6810) Thermal effects.

References and links

1. F. Krausz and M. Ivanov, "Attosecond Physics," Rev. Mod. Phys. **81**(1), 163–234 (2009).
2. J. A. Cox, W. P. Putnam, A. Sell, A. Leitenstorfer, and F. X. Kärtner, "Pulse synthesis in the single-cycle regime from independent mode-locked lasers using attosecond-precision feedback," Opt. Lett. **37**(17), 3579–3581 (2012).
3. T. Zhou, J. Ruppe, C. Zhu, I.-N. Hu, J. Nees, and A. Galvanauskas, "Coherent pulse stacking amplification using low-finesse Gires-Tournois interferometers," Opt. Express **23**(6), 7442–7462 (2015).
4. T. Udem, R. Holzwarth, and T. W. Hänsch, "Optical frequency metrology," Nature **416**(6877), 233–237 (2002).
5. B. Borchers, S. Koke, A. Husakou, J. Herrmann, and G. Steinmeyer, "Carrier-envelope phase stabilization with sub-10 as residual timing jitter," Opt. Lett. **36**(21), 4146–4148 (2011).
6. I. Thomann, E. Gagnon, R. Jones, A. Sandhu, A. Lytle, R. Anderson, J. Ye, M. Murnane, and H. Kapteyn, "Investigation of a grating-based stretcher/compressor for carrier-envelope phase stabilized fs pulses," Opt. Express **12**(15), 3493–3499 (2004).
7. T. Fordell, M. Miranda, A. Persson, and A. L'Huillier, "Carrier-envelope phase stabilization of a multi-millijoule, regenerative-amplifier-based chirped-pulse smplifier system," Opt. Express **17**(23), 21091–21097 (2009).
8. F. Lücking, V. Crozatier, N. Forget, A. Assion, and F. Krausz, "Approaching the limits of carrier-envelope phase stability in a millijoule-class amplifier," Opt. Lett. **39**(13), 3884–3887 (2014).
9. A. Baltuška, T. Fuji, and T. Kobayashi, "Controlling the carrier-envelope phase of ultrashort light pulses with optical parametric amplifiers," Phys. Rev. Lett. **88**(13), 133901 (2002).
10. R. Budriūnas, T. Stanislauskas, and A. Varanavičius, "Passively CEP-stabilized frontend for few cycle terawatt OPCPA system," J. Opt. **17**(9), 094008 (2015).
11. K. Osvay, L. Canova, C. Durfee, A. P. Kovács, A. Börzsönyi, O. Albert, and R. L. Martens, "Preservation of the carrier envelope phase during cross-polarized wave generation," Opt. Express **17**(25), 22358–22365 (2009).
12. F. Lücking, A. Trabattoni, S. Anumula, G. Sansone, F. Calegari, M. Nisoli, T. Oksenhendler, and G. Tempea, "In situ measurement of nonlinear carrier-envelope phase changes in hollow fiber compression," Opt. Lett. **39**(8), 2302–2305 (2014).
13. A. Börzsönyi, R. S. Nagymihaly, and K. Osvay, "Drift and noise of the carrier-envelope phase in a Ti:Sapphire amplifier," Laser Phys. Lett. **13**(1), 015301 (2016).
14. S. Koke, C. Grebing, B. Manschwetus, and G. Steinmeyer, "Fast f-to-2f interferometer for a direct measurement of the carrier-envelope phase drift of ultrashort amplified laser pulses," Opt. Lett. **33**(21), 2545–2547 (2008).
15. C. Li, E. Moon, H. Mashiko, H. Wang, C. M. Nakamura, J. Tackett, and Z. Chang, "Mechanism of phase-energy coupling in f-to-2f interferometry," Appl. Opt. **48**(7), 1303–1307 (2009).
16. A. M. Sayler, T. Rathje, W. Müller, Ch. Kürbis, K. Rühle, G. Stibenz, and G. G. Paulus, "Real-time pulse length measurement of few-cycle laser pulses using above-threshold ionization," Opt. Express **19**(5), 4464–4471 (2011).
17. D. C. Brown, "The promise of cryogenic solid-state lasers," IEEE J. Sel. Top. Quantum Electron. **11**(3), 587–599 (2005).

#283226 https://doi.org/10.1364/OE.25.006690
Journal © 2017 Received 19 Dec 2016; revised 5 Feb 2017; accepted 6 Feb 2017; published 14 Mar 2017

Optics EXPRESS

18. A. Borzsonyi, A. P. Kovacs, and K. Osvay, "What we can learn about ultrashort pulses by linear optical methods," Appl. Sci. **3**(2), 515–544 (2013).
19. L. Lepetit, G. Cheriaux, and M. Joffre, "Linear techniques of phase measurement by femtosecond spectral interferometry for applications in spectroscopy," J. Opt. Soc. Am. B **12**(12), 2467–2474 (1995).
20. C. Dorrer and F. Salin, "Characterization of spectral phase modulation by classical and polarization spectral interferometry," J. Opt. Soc. Am. B **15**(8), 2331–2337 (1998).
21. C. Dorrer, "Influence of the calibration of the detector on spectral interferometry," J. Opt. Soc. Am. B **16**(7), 1160–1168 (1999).
22. C. Dorrer, N. Belabas, J.-P. Likforman, and M. Joffre, "Spectral resolution and sampling issues in Fourier-transform spectral interferometry," J. Opt. Soc. Am. B **17**(10), 1795–1802 (2000).
23. www.tewati.eu
24. J. Limpert, A. Klenke, M. Kienel, S. Breitkopf, T. Eidam, S. Hadrich, C. Jauregui, and A. Tünnermann, "Performance scaling of ultrafast laser systems by coherent addition of femtosecond pulses," IEEE J. Sel. Top. Quantum Electron. **20**(5), 0901810 (2014).

1. Introduction

The spectral and temporal phase stabilities of few-cycle light pulses, most notably carrier-envelope phase (CEP), are amongst the of the most common requirements for state-of-the-art, high peak power, ultrafast laser systems. For example, CEP stability plays a crucial role in high harmonic and attosecond pulse generation [1]; while other applications, such as interferometry, coherent beam combination [2], pulse stacking [3] and precise frequency metrology [4] require all spectral phase components to be stable, including CEP and group delay (GD). The CEP stability of the most advanced Ti:Sa oscillators is now 20 mrad referring to a timing jitter of sub-10 as, obtained using a combination of feed-forward and feedback techniques [5]. Several experimental studies highlight the importance of the mechanical stability of optical elements in a chirped pulse amplification (CPA) system, especially the stretcher-compressor stages [6,7]. State-of-the-art CEP stabilization schemes for multi-kHz repetition rate CPA lasers have reduced noise below 100 mrad [8]. Conventionally, it requires a feedback loop, for example based on an acousto-optical phase shifter before or within the amplifier, which enables phase noise reduction with a defined bandwidth. However, not every solution needs a feedback loop. Certain amplifier systems can be designed such way that the seed pulses are generated through a combination of difference frequency generation and optical parametric amplification. This way passively and intrinsically phase stable pulses can be obtained [9,10]. Other nonlinear processes supporting CPA systems could potentially affect the CEP stability and needed to be addressed. For example, cross-polarized wave (XPW) generation was investigated from the point of CEP and it was shown, that this process preserves the CEP of input pulses [11]. The CEP stability of hollow fiber compression stages, which are generally used in combination with chirped mirrors to generate few-cycle NIR pulses, was also experimentally tested and found to be intensity dependent [12].

CEP stability of water-cooled Ti:Sa based amplifiers has been recently investigated and the effects of seed and pump energy, repetition rate and the cooling crystal mounts were thoroughly measured [13]. The results showed a linear dependency of the CEP noise on the pump pulse energy and no dependence on the seed energy. However, the CEP noise decreased with repetition rate, due to the decreasing time interval between consecutive pulses with increasing repetition rate. The CEP stability of entire CPA systems is generally measured using techniques such as f-to-2f interferometry [14,15] or stereo-ATI [16]. F-to-2f interferometry can be only used in case of compressed pulses and thus, cannot be utilized to measure the effects of different components on the phase inside the amplification chain of a laser system.

Obtaining high average power pulse trains based on laser materials, like Ti:Sa, leads to high thermal loads in the gain media due to the quantum defect. Temperature changes in the amplifier crystal can cause serious beam distortions, e.g. thermal lensing; thermally induced stress and birefringence in the material. These effects can be mitigated with cryogenic cooling as the thermal properties of Ti:Sa improve drastically with decreasing temperature [17]. For

Optics EXPRESS

this reason, high peak power laser systems require cryogenic refrigerators in amplifier stages to obtain high quality beams after amplification. While the thermal originated beam degradation is significantly reduced in case of cryogenic cooling, the necessary utilization of vacuum technology usually introduces severe levels of mechanical vibration into the laser system. These mechanical disturbances can affect the amplified pulses and generate spectral phase noise, which can lead to serious problems in many applications. In this work, we present an experimental study on the spectral phase noise including CEP, which originates from a cryogenically cooled Ti:Sa amplifier.

2. Experimental method and system

Spectrally resolved interferometry (SRI), a completely linear optical method, was used for the measurements as this technique measures the spectral phase noise with a detection limit of around 10 mrad for every component in an ultrafast laser system [18–22]. In principle, the absolute change of the spectral phase including the CEP in the sample arm of the interferometer can be measured with the SRI method. The measured pulse is split into two and the resulting phase difference between the two arms is determined. The majority of the measured spectral phase noise consists of GD noise, meaning that the actual measurement limit of the CEP noise can be even an order of magnitude lower than the noise of the spectral phase. The inherent noise of the SRI setup can be lowered by minimizing the path length and the number of optics in the interferometer. Based on the measured spectral phase difference between the sample and reference pulses, the definition of CEP change in the sample arm in the frequency domain can be written as

$$\Delta\varphi_{CE} = \Delta\varphi_0 - \Delta GD \cdot \omega_0, \tag{1}$$

where $\Delta\varphi_0$ is the spectral phase difference at 800 nm central wavelength, while ΔGD and ω_0 are the GD difference and the angular frequency related to the central wavelength, respectively.

The frontend of a Ti:Sa based CPA system [23] was used as the seed source of our experiment. The investigated amplifier is pumped by 150 ns FWHM pulses from a custom-made Photonics Industries DM30-527 Nd-YLF laser with an energy stability better than 0.2% RMS over long term operation. The repetition rate of the amplifier in the CPA system could be varied between single shot and 10 kHz. The double-pass Ti:Sa amplifier was built in the sample arm of the interferometer, where the amplification factor of approximately 10 was compensated by a reflective neutral density filter (NDF, 32% transmission) to match the intensity of the reference arm.

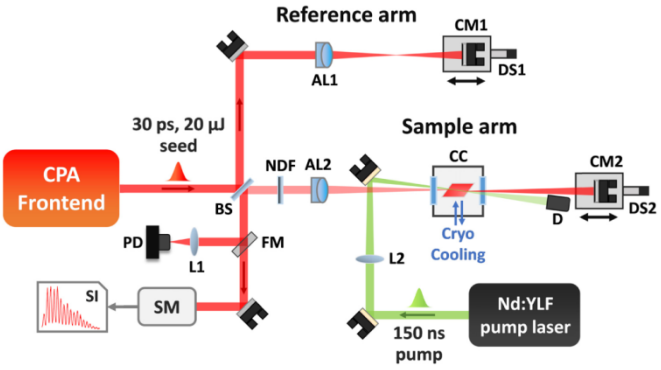

Fig. 1. Scheme of the experimental setup.

Pulses with a duration of 30 ps and an energy of 20 µJ were coupled into a Michelson interferometer (Fig. 1). A beam splitter (BS), with a measured reflection/transmission ratio of

Optics EXPRESS

70:30, splits the input seed pulse. In the sample arm, an achromatic lens (AL2, focal length 200 mm) focuses the seed into the amplifier crystal in the cryogenic chamber (CC). A concave mirror (CM2, focal length −100 mm) on a linear translator stage (DS2) is used to focus back the seed beam after the first pass to the crystal. A similar achromatic lens (focal length 100 mm) was used in the reference arm (AL1) to compensate for the material dispersion of AL2 in the sample arm, with a concave mirror (focal length −100 mm), which is placed on another translator stage (DS1). Pump pulses from the Nd:YLF laser are focused on to the Ti:Sa crystal by a single lens (L2, focal length 500 mm) while the transmitted part of the pump beam is dumped (D). The output of the interferometer is directed to the high resolution spectrometer (SM) and a flip mirror is placed before coupling into the spectrometer for measuring the gain in the double-pass amplifier by focusing the beam with a lens (L1, focal length 150 mm) on to a photodiode (PD, DET10A/M, Thorlabs). The arms of the interferometer were kept as compact as possible (0.5 m), also the height and thickness of the posts under the mirror mounts were chosen according to the requirement of increased mechanical stability of the measurement setup. The interferometer was constructed on a highly stable, research grade optical table. The complete laser system and the experimental setup was carefully covered; the flow boxes above the optical tables were shut down and the measurements were performed at night to eliminate air currents and every possible mechanical noise sources.

A Brewster-cut, uncoated, cylindrical Ti:Sa crystal with 5 mm path length, 6 mm diameter and 4.27 cm^{-1} absorption coefficient at 527 nm was mounted in a copper head attached to the cold finger of a CryoMech PT60 cryogenic refrigerator. Under operational conditions, the crystal was cooled down to <30 °K temperature. A highly compact vacuum chamber was designed and manufactured around the Ti:Sa crystal. Rubber spacers were used between the optical table and the cryogenic chamber to dampen the mechanical coupling. The chamber was evacuated to 10^{-6} mbar using a turbomolecular vacuum pump (Pfeiffer HiPace 80) and the necessary pre-evacuation of the turbo pump was performed by a Pfeiffer XtraDry 150-2 type vacuum pump, installed at a distance of 5 meters from the optical tables. The double-pass amplifier in the sample arm (Fig. 1) was driven by the same pump laser that was used for pumping the frontend amplifier. The pump pulse energy was kept at 10 mJ for all repetition rates to match the amplification factor mentioned before. The seed and pump spot sizes were closely matched in the crystal. Pumping was performed from one side of the crystal. The mechanical vibration during the experiments was monitored by an accelerometer (Hansford HS100) attached to the optical table near the interferometer. The vibrometer was calibrated to have 516.6 mV/G sensitivity. The signal was digitized using an NI USB-6009 data acquisition device and recorded on a PC. The vibration spectrum was calculated for every second, and then these spectra were averaged for a few minutes for the different circumstances.

The detection of the spectral interference fringes was performed by a homemade high resolution spectrograph, optimized for the wavelength range of 765 to 845 nm with a spectral resolution of 0.039 nm at 800 nm. The detector of the spectrograph was a triggered line scan camera (Basler spL2048-70km) with 2048 pixels and a maximal frame rate of 70 kHz, which was more than sufficient for detection in these experiments. The data acquisition from the camera was obtained using a custom in-house LabView code. The evaluation of the measured interference fringes was performed in Matlab with an algorithm based on the FFT method [19–22].

Spectral phase variations in a Ti:Sa amplifier mainly originate from refractive index variation in air (pressure and temperature changes), changes in the Ti:Sa crystal (thermal fluctuations, Kerr effect and population inversion caused by optical pumping) and the mechanical vibration of the optical elements in the setup. To minimize nonlinear phase accumulation inside the windows of the vacuum chamber and the Ti:Sa crystal, the diameter of the seed beam was decreased before the input of the interferometer to 1 mm and the

Optics EXPRESS

position of the Ti:Sa crystal was chosen so the beam diameter inside it was not less than 400 μm. Calculations confirmed that Kerr effect contributions can be neglected as the pulses are kept stretched. The refractive index change due to population inversion (i.e. pump absorption) in the crystal was also calculated for the laser parameters and the phase contribution was found negligible. As the determination of the GD from the density of interference fringes is not accurate enough to generate a proper compensation in the definition of the CEP to the φ_0 changes, the calculation of the CEP shift, as written in Eq. (1), was modified. To eliminate the effect of the GD noise, the relation between the changes of φ_0 and GD was used. Two cases can be distinguished. The only contribution to the CEP shift in the amplifier, without pumping the crystal, originates from the mechanical vibration and air movement in the optical setup whilst during pumping, the temperature fluctuation in the gain medium acts as an additional noise source. According to the previously described effects, the CEP noise of mechanical [Eq. (2)] and thermal [Eq. (3)] origin can be derived as

$$\Delta\varphi_{CE,vibrational} = \Delta\varphi_0 \cdot \left(1 - \omega_0 \frac{\Delta GD_{air}}{\Delta\varphi_{0,air}}\right) \text{and} \tag{2}$$

$$\Delta\varphi_{CE,thermal} = \Delta\varphi_0 \cdot \left(1 - \omega_0 \frac{\Delta GD_{Ti:Sa}}{\Delta\varphi_{0,Ti:Sa}}\right). \tag{3}$$

By using Eqs. (2) and (3), the CEP shift and noise could be determined only from the measured φ_0 values. This way, the error of the GD determination was mitigated, however the CEP noise of different effects can be only determined separately. In case of Eq. (2) one can derive a simple formula for GD/φ_0 the following way:

$$\frac{GD}{\varphi_0} = \frac{1}{\omega} + \frac{1}{n_{air}(\omega)} \frac{dn_{air}(\omega)}{d\omega}, \tag{4}$$

where $n_{air}(\omega)$ is the refractive index of air at a given ω circular frequency. Based on Eq. (4) a value of 424.7 as/rad for the $\Delta GD/\Delta\varphi_0$ coefficient can be calculated at ω_0 frequency, which will be experimentally tested in the following section.

3. Results

In this section, we discuss the experimental results as follows. First, the relationship between the change of GD and φ_0 is explored for the mechanical and thermal effects in our experimental arrangement. Based on these findings, we then determine the coefficients for the derivation of the CEP fluctuations from the spectral phase. Since the measurement setup needs to exhibit low inherent phase noise, next we discuss the results of measurements regarding the phase noise during each step of the starting procedure of the vacuum and cryogenic systems. With the use of the $\Delta GD/\Delta\varphi_0$ coefficients, we determine the repetition rate dependence of the thermal and mechanical originated CEP noise in the amplifier. This is followed by the discussion of the measurement results regarding the effect of amplification at this extremely low temperature. Finally, the noise spectra of the phase and mechanical vibration of the optical components will be examined.

3.1. CEP coefficients and inherent phase noise of the setup

The initial studies investigated the relation between the spectral phase and CEP. The ratio of the GD and φ_0 change was measured for the mechanical vibration dominated CEP noise determination without amplification [Eq. (2)]. The length of the Michelson interferometer was slowly changed by one of the linear translator stages. A linear fit was applied on the

Optics EXPRESS

measured $GD(\varphi_0)$ curve, which yielded a 427.1 as/rad. This result is in good agreement with the value calculated based on Eq. (4) for standard air. The coefficient in Eq. (3) was measured with the acquisition of the interference fringes of 200 Hz repetition rate pre-amplified pulses synchronized with the start of the cryogenic cooler without driving the sample amplifier with pump pulses, and finished after it reached the minimal temperature state. Similarly to the mechanical case, a linear fit was applied to the regarding temperature dependent $GD(\varphi_0)$ curve. The $\Delta GD/\Delta\varphi_0$ coefficient related to temperature changes was found to be 462.4 as/rad.

The detection limit of the experimental setup, i.e. the inherent spectral phase noise of the arrangement had to be measured. Stretched, amplified output pulses of the CPA frontend at 1 kHz repetition rate and with 16 μJ energy were injected to the interferometer. The spectral phase noise was measured without optical pumping and any vacuum devices running. 100 pulse periods were chosen from the train, which were considered long enough to calculate an instantaneous RMS value. Phase noise RMS values given in this work are the average of the RMS values calculated from the pulse periods. This average value corresponds to the center of mass of the individual histograms in Fig. 2. Multiple measurement runs were performed in all cases, where the length of a single measurement was set to 4 minutes, which corresponded to a sample number of $2.4 \cdot 10^5$. As high as 32 mrad RMS spectral phase noise was found to be present in our setup, which is represented by the grey histogram in Fig. 2 (background). The phase noise was then measured after the prevacuum pump was started and pre-turbopump vacuum level was reached. The noise increase was negligible compared to the inherent noise of the setup. However, when the turbo pump was started, had reached full operational conditions (1500 Hz rotation frequency) and the vacuum chamber was fully evacuated, the phase noise was measured again. The increased noise level was found to be 54 mrad RMS (Fig. 2, blue, vacuum). The final measurement was after the cryogenic refrigerator was started and the crystal was cooled down to the minimal temperature after 30 minutes. Under full operational conditions, with both the cryogenic cooler and vacuum pumps running, the measured phase noise increased significantly relative to the background and the vacuum level resulting in a measured RMS value of 72 mrad (Fig. 2, orange, cryo). By calculating the contributions of each operational stage relative to the background noise based on the independent noise source theorem, 43 and 47 mrad RMS spectral phase noise for the vacuum pumps and cryogenic cooler operation stage were obtained respectively. The corresponding maximal CEP noise contributions estimated from the spectral phase shifts are 0.22 and 6.3 mrad RMS for the vacuum pumps and cryogenic head, for which the measured derivatives in Eqs. (2) and (3) were used, respectively.

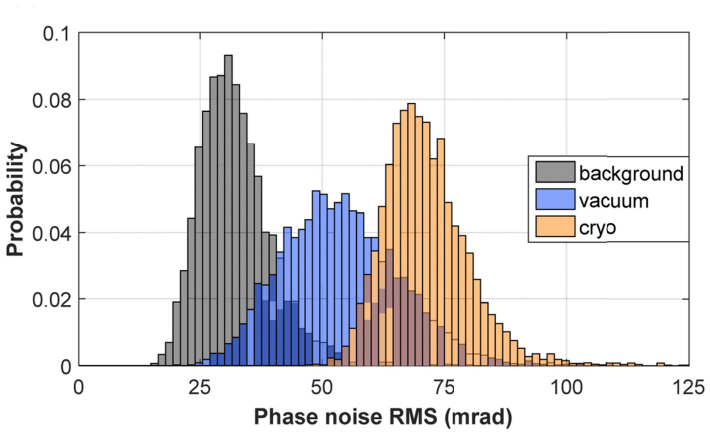

Fig. 2. Histograms of the spectral phase noise RMS without amplification for various operational stages of the experiment.

Optics EXPRESS

3.2. CEP noise of thermal and mechanical origin

After measuring the inherent phase noise, the effects of amplification on the CEP for different repetition rates (50 and 1000 Hz) were measured with similar seed pulse parameters (20 μJ energy and 30 ps stretched duration). The seed pulses in the sample arm of the Michelson-interferometer were amplified whilst the crystal was held at constant cryogenic temperature. Measurements were performed for time intervals including more than $2 \cdot 10^5$ pulses for all repetition rates, except for the 50 and 100 Hz cases, where the measurement time was decreased to 20 minutes to eliminate the effect of long term changes in the laser system. The measured fringes of unamplified cases for all repetition rates were evaluated using the derivative in Eq. (2). There was a 0.79 mrad RMS CEP noise contribution at 50 Hz, which decreased to 0.39 mrad RMS at 1 kHz repetition rate. Based on the derivative in Eq. (3), the thermal originated CEP noise contribution of the amplifier was calculated for all measured repetition rates (Fig. 3) during amplification in the sample amplifier. Figure 3 shows that the maximal thermal double pass CEP noise contribution could be measured at 50 Hz with a value of 11.5 mrad RMS, whilst there is a steady reduction in the noise level with increased repetition rate. At 400 Hz, the CEP noise dropped to 6.3 mrad RMS, and thermal originated CEP noise above 400 Hz is constant with a value of around 6 mrad. Figure 3 shows that the width of the histograms increased with lower repetition rates. This is due to the increasing time interval between the consecutive pulses at lower repetition rate and hence the CEP can drift further from pulse to pulse due to the fluctuations in the temperature of the crystal and also in air flow and mechanical noise.

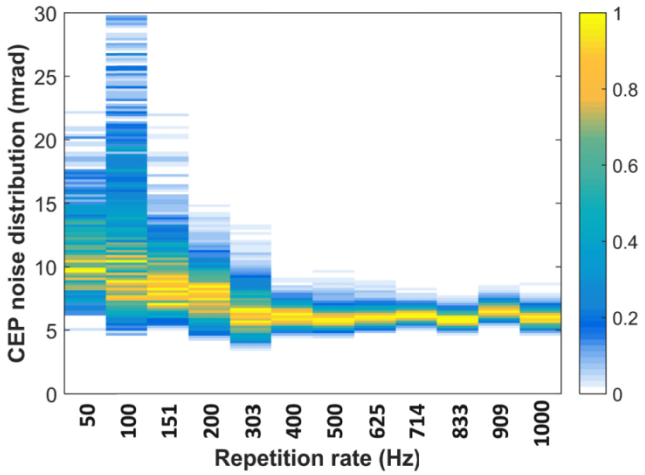

Fig. 3. Normalized thermal CEP noise histograms for different repetition rates in case of pumping with 10 mJ energy pulses.

3.3. Effect of amplification

Two experiments were performed to determine the effect of pumping the crystal on the spectral phase noise using 20 μJ, 30 ps pulses of the frontend at 200 Hz repetition rate. The cryogenic cooler was turned off during the measurement to establish the ultimate noise limit of the setup. Figure 4 shows the measured spectral phase shift for pumped and non-pumped crystals. After the cryogenic refrigerator was turned off, the phase was measured for 80 minutes and the temperature of the crystal holder mount was monitored by a thermocouple. During this period of time, a 140 °K and 124 °K increase of the mount temperature was observed for of pumped and non-pumped experiments, respectively. Figure 5 shows the computed phase noise RMS histograms for both measurements. The sensitivity of the measurement was increased by close to 20 mrad compared to the results in Fig. 2, however no

Optics EXPRESS

difference in the phase noise could be shown between the two cases. This result suggests that there are no additional phase noise effects caused by pumping under cryogenic conditions and with a highly stable pump laser. The noise of the spectral phase also did not increase with the rising temperature of the crystal mount in either case. Based on Figs. 3 and 5 we can conclude, that the determined CEP noise values of mechanical and thermal origin are worst case estimations.

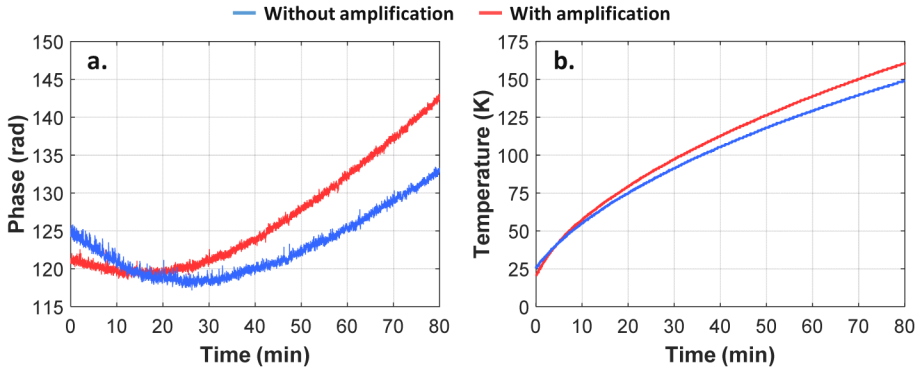

Fig. 4. Variation of the spectral phase (a) and temperature of the crystal holder (b) during warming up from cryogenic temperature in two cases: without amplification (blue) and with amplification (red).

This means, the suppression of thermal originated CEP noise in the cryogenically cooled amplifier is highly efficient compared to the water-cooled stages [13].

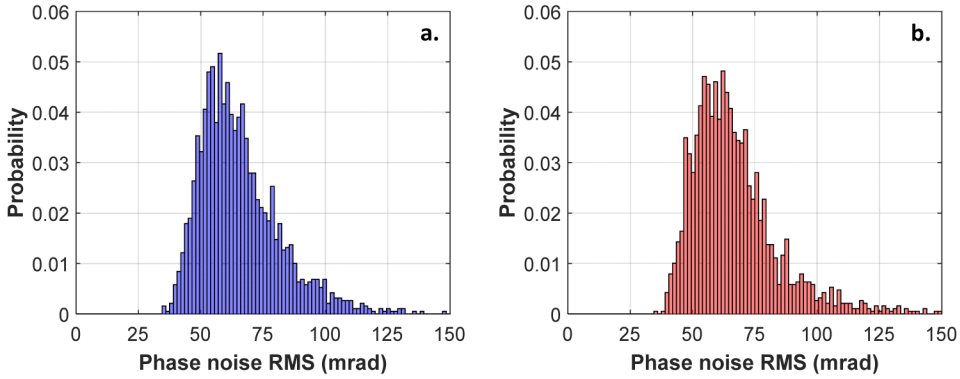

Fig. 5. Histograms of the spectral phase noise RMS in case of operation without (a) and with amplification (b).

3.4. Analysis of noise spectra

The complete understanding of the phase noise requires the measurement of mechanical vibration synchronized with the optical data acquisition enabling the identification of the mechanical noise of different components in the setup. Noise spectra were obtained by using FFT on the raw acceleration data measured by the vibrometer. The sampling frequency of the vibrometer was 24 kHz, which provided insight of the noise spectrum up to 12 kHz based on the Nyquist-Shannon sampling theorem. Figure 6 shows the vibration spectra during the background [Fig. 6, (a)], vacuum system and cryogenic refrigerator operation. The vacuum system in the setup, mainly the rotation frequency of the turbo pump (1500 Hz), and its harmonics cause the increase of mechanical noise throughout the frequency spectrum [Fig. 6, (b)]. During the startup sequence of the vacuum system, strong resonance of the mechanical components was observed around 600 Hz, which is most probably the eigenfrequency of

Optics EXPRESS

some components. However, the operation of the cryogenic refrigerator results in the vibration spectrum showing significant increase at all frequencies, particularly with a severe noise increase from 2 to 5 kHz and a few peaks below 1 kHz, which are resonances of the opto-mechanical components [Fig. 6, (c)].

The noise spectrum was also investigated in the frequency domain for optical measurements. The bandwidth in the frequency domain was increased by using a 10 kHz acquisition rate on the spectrograph and the 75 MHz pulse train from the oscillator of the CPA system. Several long measurements were performed and combined for all cases of the operational setup. This time duration (3.2 s) was the acquisition limit of the NI Max software at the 10 kHz sampling rate. The spectral phase noise spectrum up to 5 kHz frequency could still be accessed by using FFT algorithm on the phase data and Fig. 6 shows these results. The background noise phase spectrum [Fig. 6(d)] shows two strong, quite broad noise peaks around 280 and 600 Hz. Both are mechanical resonances, however only the 600 Hz peak can be detected in the mechanical spectrum (an audible noise during the start of the turbo pump). In case of the vacuum stage [Fig. 6(e)], the main new components are the rotation frequency and its harmonics. When operating the cryo cooler [Fig. 6(f)], one can see, that the level of the whole noise spectrum is increased and the broad noise increase in the range of 2-5 kHz also appears in the optical spectrum.

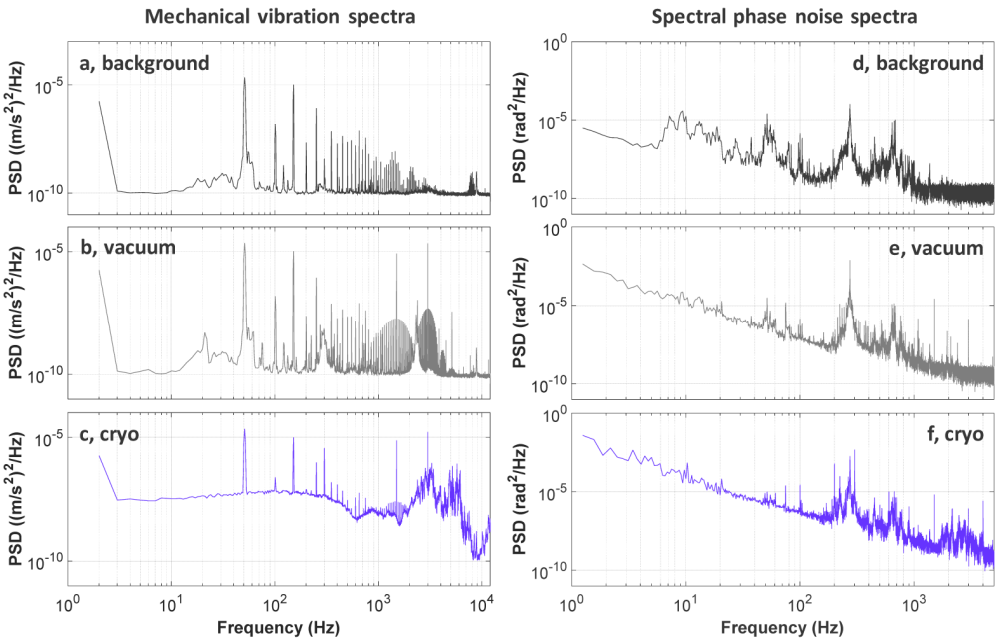

Fig. 6. Power spectral density of the noise spectra recorded with the vibrometer at different stages of starting up the experimental setup: background (a), vacuum operation (b), and the cryogenic refrigerator operation (c). Power spectral density of the noise spectra obtained from the interferometric phase measurements by FFT at different stages of starting up the experimental setup: background (d), vacuum operation (e), and the cryogenic refrigerator operation (f).

4. Summary and conclusions

A systematic investigation was presented on the noise of the spectral phase, including CEP, of laser pulses amplified in a cryogenically-cooled Ti:Sa amplifier of a CPA chain. The double-pass amplifier was built in the sample arm of a compact Michelson interferometer. The spectral phase fluctuations of stretched, broadband pulses with 800 nm central wavelength were measured by the use of the SRI method, which ensured high level of accuracy. The

Optics EXPRESS

Ti:Sa crystal was cooled below 30 °K. The inherent phase noise was measured for different operation modes, as at various repetition rates, and pump depletion. Noise contributions of the vacuum pumps and the cryogenic refrigerator were found to be 43 and 47 mrad RMS, respectively. CEP noise has been identified as having thermal as well as mechanical origin, both of which decrease with higher repetition rates. It was found, that the widths of the noise distributions broaden with lower repetition rates. The significant reduction in the thermal originated CEP noise contribution relative to room temperature cooled amplifiers makes the cryogenic cooling inevitable to reach high peak power CEP-stable pulses based on Ti:Sa technology. We have previously shown [13], that a water-cooled amplifier operating in the saturated regime does not increase the CEP noise. Based on these findings, the situation is expected to be similar for cryogenic cooling. By increasing the number of passes, however, would increase the thermal originated CEP noise, since the amplified pulse is affected by the temperature instability in the Ti:Sa crystal more times.

Spectral phase was measured with and without amplification and no significant difference in the phase noise distributions has been observed. The mechanical vibration was also measured in the setup by using an accelerometer synchronously with the optical measurements. The noise spectra of spectral phase and vibration measurements were compared and the sources of individual noise components were identified. Most significant noise sources were found to be the turbo pump, specifically the rotation frequency and its harmonics, and also the cryogenic refrigerator with a broad range of frequencies between 2 and 5 kHz.

This work highlights the sources of phase stability issues in cryogenically cooled Ti:Sa amplifiers, which are widely used in high peak and average power laser systems. The inherent CEP stability of laser systems need to be improved for many applications as stabilization loops can only eliminate noise components with a limited bandwidth. Based on our phase measurement technique, a feedback loop could be implemented to compensate for spectral phase shifts originated from the amplifier. The bandwidth of the feedback loop depends only on the electronics used for evaluation, which we estimate to be 100 Hz in the present state. By using a photodiode array in the spectrometer, a customized FPGA for evaluation and a fast actuator for control, the loop could compensate for most of the vibration below 1 kHz. However, based on our measurements, there might be not too much room for improvement in noise reduction if the entire system still exhibits over 100 mrad RMS CEP noise. In the case of coherent combination of multiple amplifier channels, the correction loop requires interferometric precision [24], for which phase instabilities have to be eliminated. For this purpose, the stability of the relative group delay of the pulses has an even higher importance, than the CEP. The accompanying mechanical vibration of the cryogenic cooling can be mitigated by using an appropriate damping between the cryogenic chamber and the optical table on which the amplifier optics are located.

Funding

The authors would like to acknowledge funding from ELI-ALPS with project number of GINOP-2.3.6-15-2015-00001 and from Laserlab Europe with grant number of EC-GA 654148 in the framework of the Horizon 2020 Programme.